Macromolecules

Article

pubs.acs.org/Macromolecules

Mechanical Properties and Cross-Link Density of Styrene–Butadiene Model Composites Containing Fillers with Bimodal Particle Size Distribution

A. Mujtaba,[†] M. Keller,[‡] S. Ilisch,[‡] H.-J. Radusch,[‡] T. Thurn-Albrecht,[†] K. Saalwächter,[†] and M. Beiner*[,†,§]

[†]Institut für Physik, Martin-Luther-Universität Halle-Wittenberg, 06099 Halle (Saale), Germany

[‡]Zentrum für Ingenieurwissenschaften, Martin-Luther-Universität Halle-Wittenberg, 06099 Halle (Saale), Germany

[§]Fraunhofer Institut für Werkstoffmechanik IWM, Walter-Hülse-Str. 1, 06120 Halle (Saale), Germany

ABSTRACT: Mechanical properties and cross-link density of model composites being solution styrene–butadiene rubbers filled with different amounts of nanosized silica particles or mixtures of nanosized silica particles and micrometer-sized borosilicate glass particles are studied. The cross-link density of the rubber matrix is measured based on a double-quantum NMR spectroscopy method. Shear data show that reinforcement and dissipation G'' in the rubber plateau range depend systematically on the total surface area of the filler per unit composite. Different contributions to reinforcement due to hydrodynamic effects, "filler network", glassy polymer layer, and "occluded rubber" are quantified based on a comparison of linear response measurements with strain sweeps performed at different temperatures. The results show a percolation threshold at silica volume fractions of about 0.15. The load-carrying capacity of the "filler network" decreases significantly with temperature. This may indicate the existence of a glassy polymer layer on the surface of the filler particles which softens several ten degrees above the bulk T_g of the rubber matrix. Two regimes are found in the dissipation above T_g which both depend systematically on the surface area of the filler system: A strongly frequency-dependent dissipation regime with power-law behavior is observed in $G''(\omega)$ at temperatures up to 70 K above the bulk T_g, and a nearly frequency-independent G'' regime dominates at higher temperatures. The molecular nature and importance of this finding for tire applications are discussed.

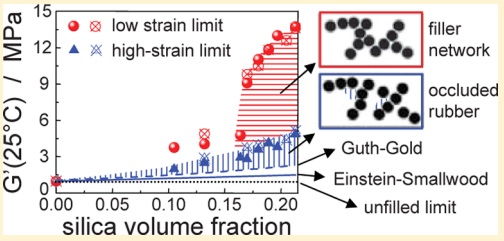

INTRODUCTION

Elastomers containing nanosized fillers like carbon black, silica, or layered silicates with large specific surface area are of central importance for various fields of application. A standard application, where such composite materials are used from the very beginning, is tires. In particular, the optimization of elastomer nanoparticle composites for tire treads is a classical problem and of major importance for the performance of tires.[1−6] This is a multiparameter optimization problem since rolling resistance, wet grip, abrasion, and other properties result in different requirements regarding the mechanical properties of an elastomer nanoparticle composite. Most relevant for wet grip and rolling resistance is the dissipation in different frequency ranges.[7−9] While the wet grip is determined by the relaxation behavior at high frequencies and small-strain amplitudes, the rolling resistance is, according to experimental studies on realistic road surfaces and related simulations, connected with the dissipation at lower frequencies.[10−12] Although this has been known for decades, a predictive understanding of the parameters influencing application relevant quantities like fuel consumption, CO_2 emission, abrasion, or braking behavior of tires is still missing. The optimization is often done based on existing experience, empirical rules, and extended screening experiments. This is due to the fact that there are various effects on the microscopic scale influencing the dissipation behavior in parallel which are still not well understood from the scientific point of view. The optimization of composites for tire applications touches fundamental scientific questions in the field of soft-matter science like those for the origin of the glass transition,[13−20] the influence of spatial confinement effects,[21−24] constraints at interfaces,[25−29] and network topology[30,31] on the dynamics of polymers. This shows nicely that there is a close relation between basic research in the field of soft matter science and traditional applications of filled elastomers in tires. From that perspective it seems important to understand and quantify effects influencing the relaxation dynamics of filled elastomers based on model systems and modern techniques to characterize network topology, mesostructure, and dynamics of composite materials.

In this paper we report results from studies on two series of model systems based on a recently developed solution styrene–butadiene rubber filled with either different amounts of nanosized silica particles or mixtures of nanosized silica and micrometer-sized borosilicate particles. This allows to investigate systematically the influence of the filler system on the

Received: May 9, 2012
Revised: July 8, 2012
Published: July 31, 2012

   dx.doi.org/10.1021/ma300925p | *Macromolecules* 2012, 45, 6504–6515

Table 1. Sample Formulations and Network Properties

	label	sulfur (phr)	U7000GR (phr)	BK3 (phr)	ϕ (vol %)	$D_{res}/2\pi$ (kHz)	defects (%)	ν (10^{26} m^{-3})
unfilled	X0.9	1.26				0.2258	5.8	2.32
	X1.0	1.4				0.2465	4.2	2.53
	X1.1	1.54				0.2598	4.8	2.67
	X1.2	1.68				0.2683	5.9	2.76
series I: composites filled with silica U7000GR	Si20	1.4	20		0.075	0.2067	10.1	2.12
	Si30	1.4	30		0.105	0.1831	12.2	1.88
	Si40	1.4	40		0.132	0.1757	13.0	1.81
	Si60	1.4	60		0.156	0.1470	26.9	1.51
	Si64	1.4	64		0.165	0.1455	27.0	1.50
	Si68	1.4	68		0.173	0.1445	27.6	1.48
	Si72	1.4	72		0.181	0.1436	27.9	1.47
	Si80	1.4	80		0.213	0.1399	27.4	1.44
series II: composites filled with U7000GR + BK3	BK40	1.4	40	40	0.201	0.1730	28.5	1.78
	BK20	1.4	60	20	0.208	0.1451	28.4	1.49
	BK12	1.4	68	12	0.210	0.1428	27.8	1.47
	BK08	1.4	72	08	0.212	0.1402	27.0	1.44
	BK00	1.4	80	00	0.213	0.1399	27.4	1.44

cross-link density of the polymer network, on the percolation of the solid "filler network" as well as its consequences for the frequency−temperature-dependent dissipation of advanced composite materials. Although the studied samples are not directly designed for a special application, a systematic study should help to gain deeper insights into phenomena determining the properties of filled elastomers and potentially contribute to a more efficient optimization of such materials.

EXPERIMENTAL SECTION

Samples. Solution styrene−butadiene rubber (Sprintan SLR-4602 - Schkopau from Styron Deutschland GmbH) filled with two types of particles with significantly different specific surface area have been investigated. Unfilled rubbers are used as a reference to estimate cross-link densities in absolute units. Sprintan SLR-4602 - Schkopau contains 21 wt % styrene, its vinyl level is 63%, and its T_g is −25 °C.[32] Series I consists of composites containing 0−80 phr (parts per hundred rubber) of silica (Ultrasil U7000GR from Evonik Industries AG with a BET surface area of 175 m^2 g^{-1}),[33] corresponding to filler volume fractions $0 < \phi_{U7000GR} < 0.21$. Series II consists of composites filled with mixtures of U7000GR silica and foamed borosilicate glass particles (Trovo powder BK3 from Trovotech GmbH with an average particle size of about 3 μm and a BET surface area of 3−20 m^2 g^{-1}).[34] The filler volume fraction in series II is kept constant ($\phi \approx 0.21$). The sample formulations are summarized in Table 1. 3-Octanoylthio-1-propyltriethoxysilane (NXT Silane from Momentive Inc.) grafting on the silica surface is used to reduce the filler−filler interaction and to get well-dispersed silica. Oil, sulfur (cf. Table 1), zinc oxide (2.5 phr), stearic acid (1 phr), *N*-cyclohexyl-2-benzothiazole sulfenamide (CBS, 1.5 phr), and diphenylguanidine (DPG, 1.5 phr) are further additives used in all samples. By varying the silica U7000GR content in series I, the ratios silica to silane (0.121 phr silane per 1 phr U7000GR) and silica to oil (0.25 phr oil per 1 phr filler) are kept constant. In series II the ratio filler to silane to oil is always the same (0.121 phr siliane and 0.25 phr oil per 1 phr filler). In the case of unfilled compounds with different vulcanization systems a one-step mixing process with an initial temperature of 50 °C and 60 rpm rotor speed for 10 min was used. Compounds containing filler are manufactured applying a two-step mixing process. In the first mixing step, a starting temperature of 125 °C was chosen in order to guarantee that silanization can take place at a temperature higher than 140 °C for 4 min. The rotor speed during that mixing step was 60 rpm, and the mixing time was 15 min. In the second mixing step, the vulcanization system was added at an initial kneader temperature of 50 °C, a rotor speed of 50 rpm, and 5 min mixing time. All rubber compounds are finally vulcanized at 160 °C in a compression molding machine. The pressing time was chosen in accordance with vulcanization times t_{90} determined from dynamic vulcameter measurements.[35]

Dynamic Mechanical Analysis. The dynamic shear modulus $G^*(\omega,T)$ was measured in a wide frequency−temperature range with a Rheometrics RDAII instrument using a control strain of 0.2%. This strain is in the linear response range as confirmed by strain sweeps. Measurements are performed on as-prepared samples with rectangular geometry having average dimensions of 20 × 10 × 2 mm^3. Temperature sweeps were measured from −70 to 150 °C with a temperature increment of 3 K and 60 s of soak time. Three data points (ω = 1, 10, and 100 rad/s) were taken at each temperature. Frequency sweeps in the range 0.1−100 rad/s with five points per decade were carried out at temperatures between −35 and 150 °C to construct master curves. Soak time for each temperature was 600 s, and temperature increment was 3 K. For nonlinear mechanical analysis, strain induced softening phenomena (Payne effect) were studied using an Anton Paar MCR501 rheometer with strain amplitudes in the range from 0.001 to 20%. Isotherms were measured at an angular frequency ω = 10 rad/s after 600 s soak time.

Double-Quantum NMR Measurements. To determine the average cross-link density of our composite materials, double-quantum NMR experiments[30] were carried out at 120 °C on a Bruker minispec mq20 spectrometer operating at 0.5 T (20 MHz). The 90° and 180° pulses had a length of 1.7 and 3.5 μs, respectively. The dead time was 12 μs. Quantitative double-quantum (DQ) or, more generally, multiple quantum (MQ) NMR is a powerful method to measure the cross-link density of polymer networks by detecting weak residual dipolar coupling.[36] The existence of cross-links in rubber matrices gives rise to the nonisotropic fast segmental motions of polymer chains. Because of nonisotropy of chain segmental fluctuation, dipole−dipole couplings between the protons in the monomeric units are not averaged out (as it is the case in isotropic low molecular mass liquids), but a residual dipolar coupling prevails. This residual dipolar coupling is proportional to the network cross-link density. DQ NMR spectroscopy generates two qualitatively different signal components. A buildup curve (I_{DQ}) dominated by spin-pair double-quantum coherences and a decay curve (I_{ref}). The sum of both components (I_{DQ} + I_{ref}) contains the full magnetization of the sample, i.e., contributions from dipolar coupled network segments and contributions from uncoupled units (isotropically mobile network defects, e.g., dangling ends, loops, oil content). Dipolar coupled segments (network) exhibit nonexponential faster relaxation while the signal from uncoupled parts appears in the form of slower exponential decay (Figure 1a).

In order to correct the raw I_{DQ} buildup data shown in Figure 1a for the obvious long-time relaxation effects and enable a quantitative

dx.doi.org/10.1021/ma300925p | Macromolecules 2012, 45, 6504−6515

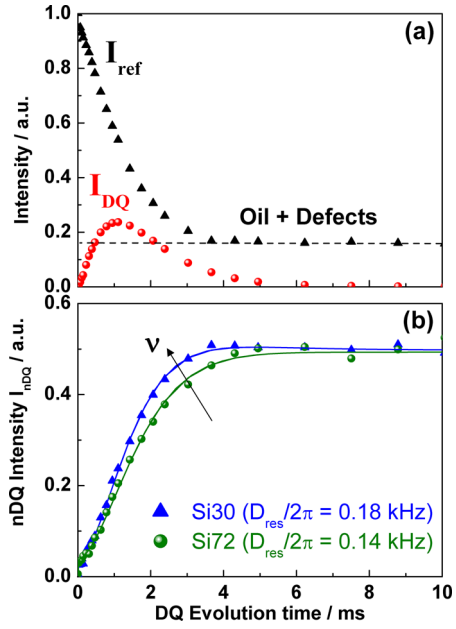

Figure 1. (a) DQ buildup (I_{DQ}) and reference decay (I_{ref}) data as a function of the double-quantum evolution time τ_{DQ}. $I_{ref} - I_{DQ}$ can be used to highlight the nonelastic, slowly relaxing (isotropically mobile) defect fraction. (b) Normalized buildup curves (I_{nDQ}) as a function of t_{DQ}. The solid lines are fits based on eq 2 assuming a Gaussian distribution of dipolar couplings.

analysis, it is divided point-by-point by a suitable relaxation-only function, $I_{\Sigma MQ}$. This function is the sum of the mentioned ($I_{DQ} + I_{ref}$) sum function, and in order to obtain it, the mentioned defect fraction has to be subtracted:

$$I_{\Sigma MQ} = I_{DQ} + I_{ref} - B \exp(-2\tau_{DQ}/T_2^*) \quad (1)$$

The defect fraction with relative amplitude B is easily identified by an exponential fit to the data range where I_{DQ} has essentially decayed to zero (i.e., beyond a DQ evolution time of about 8 ms). Now, the DQ buildup data can be normalized, obtaining $I_{nDQ} = I_{DQ}/I_{\Sigma MQ}$. I_{nDQ} is independent of temperature-dependent relaxation (decay) effects, and it is dominated by the dipolar interactions that are only related to the network structure. In the absence of relaxation effects of nonelastic network defects, I_{nDQ} (Figure 1b) can be evaluated under the assumption of a Gaussian distribution of dipolar couplings according to

$$I_{nDQ}(\tau_{DQ}) = \frac{1}{2}\left(1 - \frac{\exp\left\{-\frac{\frac{2}{5}D_{res}^2\tau_{DQ}^2}{1+\frac{4}{5}\sigma^2\tau_{DQ}^2}\right\}}{\sqrt{1+\frac{4}{5}\sigma^2\tau_{DQ}^2}}\right) \quad (2)$$

The values of residual dipolar coupling D_{res} (Table 1) are proportional to the cross-link density ν of the polymer network. The parameter σ represents the distribution width in an inhomogeneous sample, which for the case of SBR is dominated by "spin inhomogeneity" related to the copolymer character of SBR.[31] The ratio σ/D_{res} is found to be nearly constant at a value of around 0.35 ± 0.05 for all samples. Experimental D_{res} values are used in this paper to study the influence of filler content and surface area on the cross-link density of the rubber matrix in composite materials.

RESULTS

DQ NMR spectroscopy measurements on unfilled rubbers with variable content of cross-link agent and cross-link density allow, in combination with shear measurements on these samples, to estimate the cross-link density ν of rubbers in absolute units. According to classical theories describing rubber elasticity, the cross-link density ν can be estimated from the plateau modulus G_N^0 of unfilled elastomers[37]

$$G_N^0 = \nu kT \quad (3)$$

The plateau modulus G_N^0 can been taken from temperature-dependent shear data as shown in Figure 2a using fits based on eq 3. Note that the storage moduli $G'(T)$ for all unfilled samples are in line with this most simple theoretical approach. The D_{res} values from independent DQ NMR measurements on unfilled rubbers are proportional to the ν values determined from shear data (Figure 2b). This allows to determine the proportionality constant between both quantities being A_{NMR} = 1.027 × 10^{27} m^{-3}/kHz for our Sprintan SLR-4602 - Schkopau samples with a specific microstructure (21 wt % styrene content, 63% vinyl level). Based on this independently determined constant, the cross-link density ν of composite materials containing the same rubber matrix can be estimated in absolute units ($\nu = A_{NMR}D_{res}/2\pi$) subject to the constraint that the simplistic assumptions leading to eq 3 are correct. This is an interesting and novel method enabling us to quantify effects caused by changes of the cross-link density of the polymer matrix in composites.

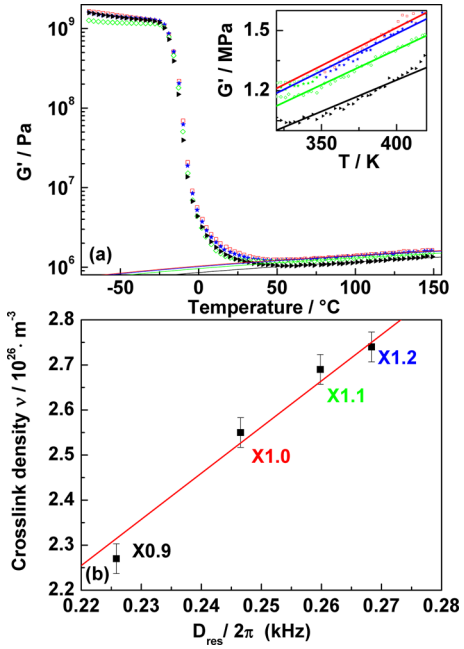

Figure 2. (a) Temperature dependence of storage (G') and loss (G'') part of the dynamic modulus of four unfilled, differently cross-linked samples. Angular frequency of the measurements is ω = 100 rad/s. The lines are linear fits to the rubber plateau in $G'(T)$ based on eq 3. (b) Cross-link densities ν obtained by dynamic shear measurements as a function of D_{res} from DQ NMR measurements. The line is a linear fit to the data ν = 1.027 × 10^{27} m^{-3}/kHz·($D_{res}/2\pi$), allowing to estimate the cross-link density of composites in absolute units based on DQ NMR measurements.

DQ NMR measurements for the two composite series show that the cross-link density of the rubber matrix depends systematically on filler content and composition of the U7000GR/BK3 filler system (Figure 2). The D_{res} values being proportional to the cross-link density of the polymer matrix are ∼45% reduced for composites containing 80 phr

dx.doi.org/10.1021/ma300925p | Macromolecules 2012, 45, 6504−6515

silica U7000GR compared to unfilled elastomers (Table 1). The D_{res} values show a systematic decrease with increasing silica U7000GR content. A similar trend occurs if the U7000GR content is reduced but substituted by significantly larger BK3 particles at fixed overall volume fraction of the filler $\phi = \phi_{U7000GR} + \phi_{BK3} \approx 0.21$. The additional BK3 fraction has obviously a negligible influence. This observation indicates that the total surface area of the filler system per unit composite, related to the size of the filler particles, is responsible for the observed reduction of the cross-link density ν, in agreement with previous, more qualitative observations.[31]

Temperature-dependent shear measurements on series I with composites containing different amounts (0−80 phr) of silica U7000GR are presented in Figure 3. A glass to rubber

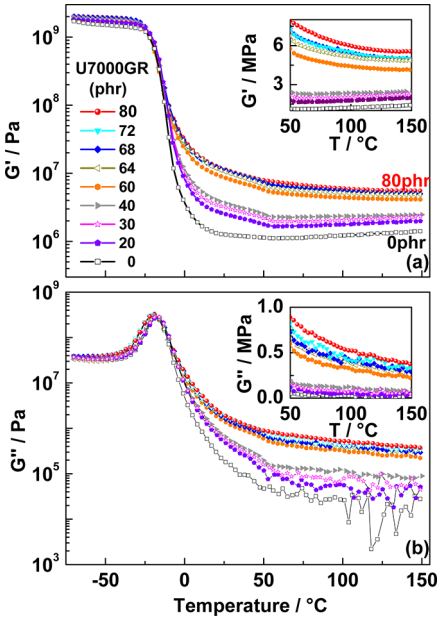

Figure 3. Temperature-dependent shear (a) storage and (b) loss modulus of composites filled with 0−80 phr silica U7000GR. Measurements are done at 0.2% strain amplitude and at an angular frequency of 100 rad/s. Insets show a linear representation of G' and G'' in the temperature range 50−150 °C.

transition appears for all samples at about −20 °C. The temperature-dependent storage modulus G' in the plateau region at $T > 50$ °C shows a clear decrease of reinforcement with decreasing filler content (Figure 3a). This effect seems to be less pronounced at low U7000GR contents <50 phr compared to the changes observed at high silica contents >50 phr. One possible interpretation of this behavior is that there is a certain fraction of the rubber matrix which has a significantly higher softening temperature than bulk rubber. Consistent with this finding in the storage modulus G', there are strong contributions to the loss modulus G'' in the plateau range for filled elastomers significantly above the maximum in $G''(T)$, indicating the α relaxation of the polymer matrix. It is important to note that G'' in the plateau range is strongly increasing with the U7000GR content. This is application relevant, since dissipation in this range is important for the rolling resistance of tires. Figure 4 shows master curves constructed by horizontal shifting from isothermal frequency sweeps for series I measured every 3 K at temperatures between −35 and 150 °C. The master curves confirm nicely the trends

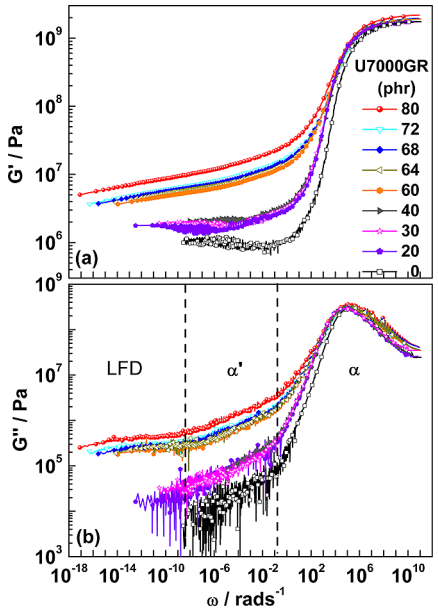

Figure 4. Master curves of (a) storage and (b) loss modulus for composites containing different amounts (0−80 phr) of silica U7000GR. The original isotherms are only horizontally shifted. Three different dissipation regimes in the loss modulus at different frequencies are indicated by labels corresponding to α peak, α' wing, and low-frequency dissipation (LFD) regime. Reference temperature is 0 °C.

seen in isochronal sweeps and indicate that the time temperature superposition principle is apparently not violated in the investigated frequency temperature range. At frequencies slightly below the α relaxation, a strong α' wing appears in a log G'' vs log ω plot before a low-frequency dissipation (LFD) regime with nearly constant G'' values is reached. A systematic reduction of G'' with decreasing silica content is also observed in case of the master curves. Systematic trends and peculiarities in the shift factors a_T (cf. Appendix, Figure 13a) show, however, that the temperature dependence of different regions of the relaxation spectrum (α, α', LFD) is most likely not identical. The shift factors measured for filled samples must thus be considered apparent quantities. The tan δ curves presented in Figure 14a of the Appendix do also indicate the existence of α' and LFD regions for samples with higher silica U7000GR contents as discussed above.

Shear data for composites, where silica U7000GR is partly substituted by large borosilicate glass particles BK3 (Figure 5), show similar trends like those for composites with variable content of U7000GR. The G' values in the rubber plateau range seem to be mainly determined by the U7000GR content. The additional BK3 fraction does not cause significant extra reinforcement. The temperature dependence of the storage modulus G' shows similar peculiarities like those observed for series I. Strong temperature-dependent changes above the α relaxation and a weak temperature dependence above $T = 50$ °C are observed in $G'(T)$. Correspondingly the loss modulus G'' is characterized by a significant shoulder slightly above T_α and weaker, only slightly temperature-dependent contributions at high temperatures. These results from isochronal measurements at constant frequency ($\omega = 100$ rad/s) are consistent with effects seen in master curves constructed from isotherms (Figure 6) measured in a wide temperature range (−35 to 150 °C). The time-temperature superposition principle seems to be

dx.doi.org/10.1021/ma300925p | Macromolecules 2012, 45, 6504−6515

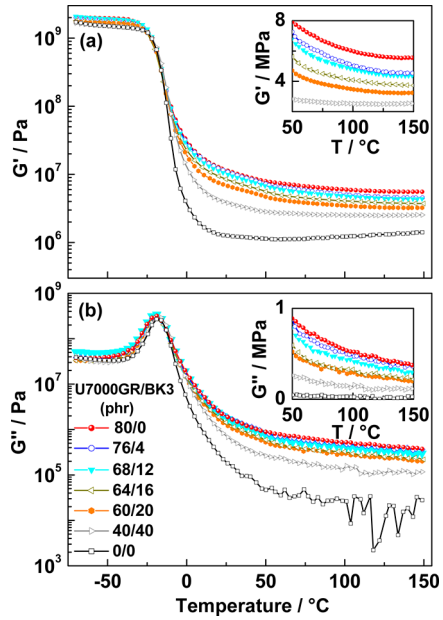

Figure 5. Temperature-dependent shear (a) storage and (b) loss modulus of composites filled with mixtures of U7000GR silica and borosilicate BK3 particles. The total filler content is 80 phr in all samples. The degree of substitution of silica by BK3 (in phr) is specified in the legend. Measurement frequency is 100 rad/s. Insets show a linear representation of G' and G'' in the temperature range of 50−150 °C.

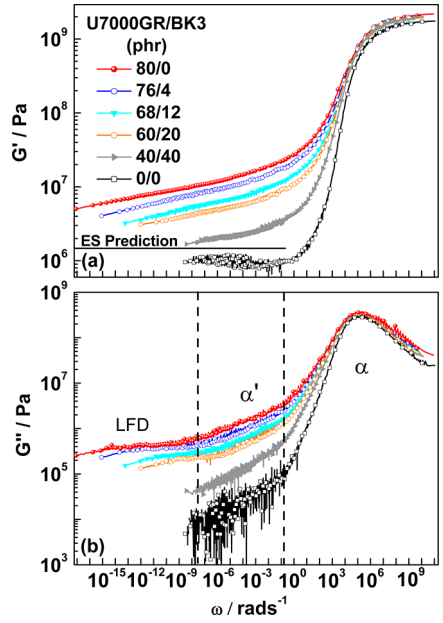

Figure 6. Master curves of shear (a) storage and (b) loss modulus for composites containing different mixtures of silica and borosilicate BK3 particles. The degree of substitution of silica by BK3 (in phr) is specified in the legend. The original isotherms are only horizontally shifted. Three different dissipation regimes in the loss modulus at different frequencies are indicated by labels corresponding to α, α', and low-frequency dissipation (LFD) regime. The reference temperature is 0 °C. The ES prediction for the storage modulus in the plateau range at the highest temperature used in the master curves 150 °C is indicated by a thin line in (a).

also applicable for composites containing mixtures of two different fillers. Besides the conventional α peak, an α' wing and frequency-independent low-frequency dissipation (LFD) contributions are seen for samples with higher U7000GR content just as discussed above for series I without additional BK3 content. The shift factors a_T (cf. Appendix, Figure 13b) indicate again that the temperature dependencies of α, α', and LCD region are different. The tan δ curves shown in Figure 14b of the Appendix confirm the existence of α' and LFD regions for higher silica contents.

A parameter explaining the similarity of the observations for composites with variable U7000GR content (series I) as well as those where U7000GR is partly substituted by BK3 (series II) seems to be the total surface area of the filler system per unit composite which should be dominated by the U7000GR silica fraction. This idea is nicely confirmed by a direct comparison of shear curves for a sample containing 60 phr U7000GR (ϕ = 0.156, $\phi_{U7000GR}$ = 0.156) with those containing 60 phr U7000GR plus 20 phr BK3 (ϕ = 0.208, $\phi_{U7000GR}$ = 0.162) (Figure 7). Storage and loss modulus of both samples seem to coincide nearly perfectly supporting the minor importance of the BK3 fraction for reinforcement and dissipation, respectively.

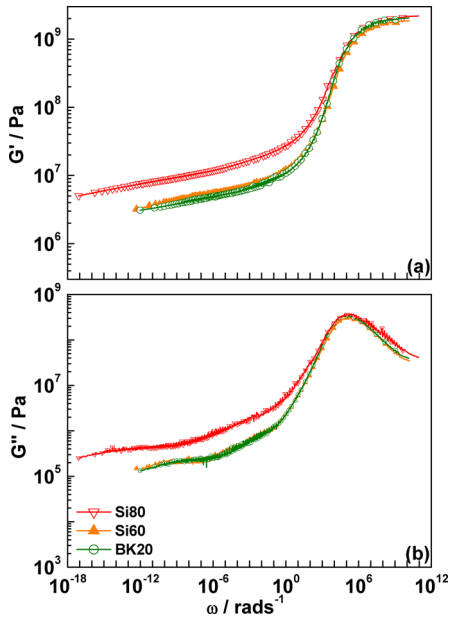

Figure 7. Comparison of master curves of shear (a) storage and (b) loss modulus for sample Si60 containing 60 phr silica (up triangle) and sample BK20 containing 60 phr silica plus 20 phr borosilicate BK3 (circles) with data for sample Si80 filled with 80 phr silica (down triangles).

A standard technique to quantify the contributions of the so-called "filler network" formed by a percolating solid phase incorporating the filler particles in composite materials are strain sweeps which are performed at different temperatures on as-prepared samples. Results from shear measurements at 25 °C with strain amplitudes γ increasing from 0.001 to 20% show a sigmoidal decrease of the storage modulus $G'(\gamma)$. This effect occurs similarly for samples with variable silica content (Figure 8a) as well as samples where the U7000GR particles are partly substituted by larger BK3 particles (Figure 8b). Strain sweeps measured at 60 °C for series I containing different amounts of U7000GR are presented in Figure 8c and show a significant but less pronounced sigmoidal decrease. This strain induced

dx.doi.org/10.1021/ma300925p | Macromolecules 2012, 45, 6504−6515

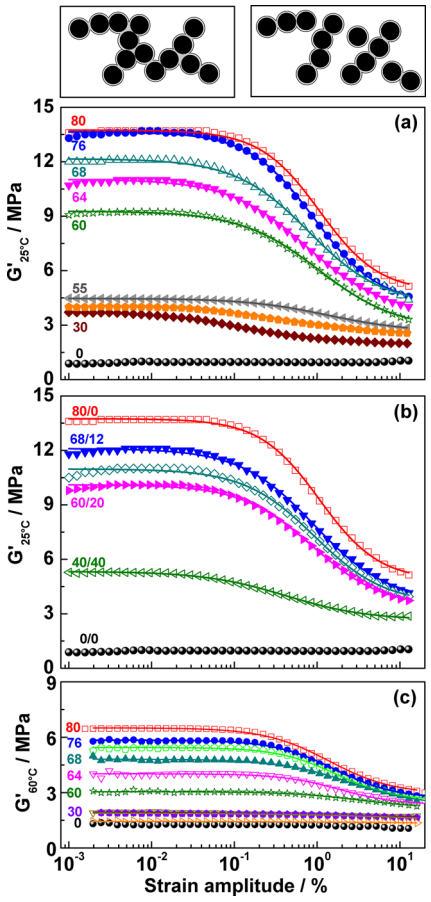

Figure 8. Storage modulus G' versus shear strain amplitude γ (Payne effect) for composites containing (a) different amount of silica and (b) mixtures of silica U7000GR and borosilicate BK3. Measurements are performed at 25 °C and 10 rad/s. The lines are fits based on the Kraus equation (eq 4). Part c shows data for samples with different U7000GR content measured at 60 °C and 10 rad/s. The top insets show sketches of the filler network before ($\gamma \rightarrow 0$, left) and after applying large deformations ($\gamma \rightarrow \infty$, right).

softening phenomenon is called Payne effect[38] and can be approximated by the Kraus equation[39]

$$G'(\gamma) = G'_{\infty} + (G'_0 - G'_{\infty})/(1 + (\gamma/\gamma_c)^{2m}) \quad (4)$$

where γ is the shear strain amplitude, γ_c is the critical strain amplitude defining the breakdown of the filler network, m is a phenomenological exponent, and G'_0 and G'_{∞} are the limiting values of $G'(\gamma)$ for small- and large-strain amplitudes γ, respectively. The solid lines in Figure 8 represent fits based on eq 4. In all cases the main change in G' occurs at a critical strain of about $\gamma_c \approx 1\%$ (Figure 8a–c). The step height $\Delta G' = G'_0 - G'_{\infty}$ in strain sweeps is commonly more pronounced for large U7000GR filler contents and tends to disappear for small U7000GR fractions $\phi < 0.15$ (<55 phr). This finding is similar to percolation thresholds for other silica filled polymers at about $\phi \approx 0.11$ ($\approx$ 40–45 phr) reported in the recent literature.[40,41] Note that the modulus step height $\Delta G'$ is similar for series I and II if the silica U7000GR content is larger than 0.15 (>55 phr). The "filler network" seemingly percolates at 25 °C in both series for such U7000GR contents (sketch in the top left inset of Figure 8) independent of the additional BK3 fraction in series II. The $\Delta G'$ values for U7000GR contents $\phi_{U7000GR} < 0.15$ (<55 phr) are significantly smaller in series I, indicating that the filler particles in these samples do not percolate although bigger filler aggregates should be still present. A direct comparison with the behavior of BK3 substituted samples in this range is unfortunately not possible since composites with BK3 contents >40 phr are hard to prepare. Interestingly, the step height $\Delta G'$ is significantly (about 50%) reduced in case of strain sweeps measured at 60 °C compared to room temperature data. This shows clearly that the contributions of the filler network to reinforcement are less pronounced at high temperatures.

Additional insights come from a detailed comparison of isochronal shear measurements performed with different strain amplitudes on as-prepared samples. Measurements performed on a composite containing 80 phr silica U7000GR (i) with small-strain amplitude (γ = 0.2%), (ii) with large-strain amplitude γ = 9%, and (iii) with small-strain amplitude γ = 0.2% after initial deformation with a strain amplitude of γ = 15% at T = 25 °C are compared in Figure 9. Large-strain

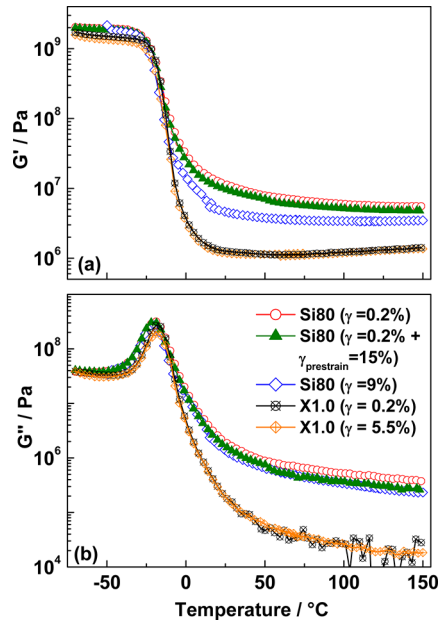

Figure 9. Temperature dependence of shear (a) storage and (b) loss modulus from measurements with small-strain amplitudes (open circles) and large-strain amplitudes (open diamonds) for a composite containing 80 phr silica. An additional measurement with small-strain amplitude (full triangles) was performed after applying an initial prestrain of γ = 15% at T = 25 °C. Measurements frequency is 100 rad/s. Corresponding data for an unfilled sample are also presented (crosses at center).

measurements show significantly lower $G'(T)$ values in the entire temperature range above the α relaxation compared to the other two perturbations. Interestingly, the difference between the G' values measured with large- and small-strain amplitudes is significantly larger around room temperature compared to the situation at high temperatures around 150 °C (Figure 9). This is also confirmed by strain sweeps performed at different temperatures on as-prepared samples. All these results show that the Payne effect is less pronounced at high temperatures and indicate that the corresponding "filler network" has a smaller load-carrying capacity. The small difference between small-strain measurements with or without prestrain of 15% may be a sign for fast recovery processes leading to a reformation of the filler network after a single large-

dx.doi.org/10.1021/ma300925p | Macromolecules 2012, 45, 6504–6515

amplitude deformation. This recovery process might be nearly completed before temperature-dependent measurements with small-strain amplitude are performed subsequently. The storage modulus of unfilled samples is practically unaffected by the strain amplitude comparing the temperature scans with γ = 0.2% and 5.5% (Figure 9). This finding is in agreement with the absence of the Payne effect in the strain sweeps of unfilled rubbers (Figure 8) and supports the relevance of the "filler network" for strain-dependent effects in highly filled samples. Interestingly, the differences between the loss modulus values $G''(T)$ of the composite containing 80 phr silica U7000GR measured using different strains are less pronouced. The loss modulus curves measured under different conditions in the range of the α process are very similar. Certain differences between differently measured composites appear only at high temperatures where the dissipation is slightly higher for that sample which has never been exposed to large ampltiude deformation, i.e., for that sample where the "filler network" should be intact. In case of unfilled rubbers the dissipations $G''(T)$ obtained using small- and large-strain amplitudes are weak and practically identical in the entire temperature range.

DISCUSSION

Cross-Link Density of Rubber Matrices in Composites. Our study nicely demonstrates that the cross-link density of the polymer matrix of filled elastomers can be estimated in absolute units combining DQ NMR measurements with shear measurements on unfilled reference samples. The results for two series of differently filled composites show clearly that the average cross-link density ν decreases systematically with increasing content of nanosized U7000GR silica particles (Figure 10). A

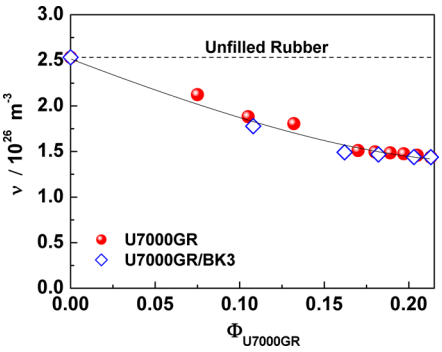

Figure 10. Cross-link densities as a function of silica U7000GR content for series I containing only silica (circles) and series II containing mixtures of silica U7000GR and borosilicate BK3 particles (diamonds).

reduction of about 45% is obtained for technical relevant filler contents of about 80 phr compared to unfilled samples with otherwise identical composition. Additional micrometer-sized BK3 filler particles seem to be of minor importance for this effect and do not influence the cross-link density significantly. This is an interesting result showing that nanosized filler particles do not act as physical cross-linker or that there is at least a molecular mechanism which overcompensates this effect and results in an effectively reduced cross-link density. A straightforward interpretation of this finding is to assume that the cross-linking agent is partly deactivated by absorption on the large surfaces of the filler particles. Accordingly, the total surface area per unit composite would be the main parameter influencing the average cross-link density. Note that a certain reduction of the cross-link density has been recently also reported for sulfur-vulcanized natural rubber clay composites and related to absorption effects, decreasing the vulcanization efficiency.[31] The observations for our composite materials might be understood as further evidence for an absorption of cross-linking agents at filler surfaces. The presented results show nicely that modern DQ NMR methods are an excellent approach to study and control this rather pronounced effect.

Changes in the cross-link density due to the presence of nanosized filler particles are often expected to have a considerable influence on the mechanical properties of filled elastomers and their optimization for special applications. The presented DQ NMR method opens an interesting way to quantify the influence of this effect on the mechanical properties of composite materials. In particular, this novel approach allows separating property changes due to cross-link density from other effects which do occur in parallel if the filler content is varied. Our results clearly indicate that the average cross-link density of the polymer matrix is significantly reduced with increasing the specific surface area of the filler system. The storage modulus G' in the plateau range, however, is systematically increasing with increasing surface area of the filler system. Obviously, reinforcement effects caused by the filler overcompensate the small modulus changes caused by the variation of the cross-link density. This is expected and easy to understand comparing the changes in the plateau modulus due to the filler content (Figures 3 and 5) with small variations of G_N^0 which are observed based on a change of ν by 20% in unfilled rubber (Figure 2).

Another interesting aspect is a possible influence of the elastomer network topology on the dissipation G'' of composite materials. There is clear evidence that the dissipation G'' in plateau range increases systematically with increasing U7000R filler content (Figures 3 and 5). At the same time the cross-link density decreases. A similar trend in G'' is not observed for unfilled samples with cross-link densities varied in the same range. Such systems show always a low dissipation G'' at 60 °C of about 1×10^4–5×10^4 Pa. The defect contributions in the DQ NMR signal is systematically increasing with the silica U7000GR content in series I without BK3 but nearly constant for series II containing mixtures of silica U7000GR and BK3 particles (Table 1). This indicates that the oil content is mainly responsible for the observed changes in the defect values. Otherwise, the dissipation G'' is changing for series II although the defect values are practically constant showing that the oil content is not responsible for the systematic changes in G'' with composition. Finally, we conclude that the high dissipation in the plateau range of the composites is mainly related to the presence of nanoscopic U7000GR filler particles and neither due to changes of the topology of the elastomer network nor due to the oil content. This is a novel, application-relevant information and interesting since the dissipation G'' in plateau range is of central importance for filled elastomer used as tire tread and the rolling resistance of entire tires (technically often quantified by tan δ at 60 °C and 10 Hz).[42,43]

Effects Contributing to Reinforcement. An important issue for understanding the mechanical properties of filled elastomers is the molecular origin of the large reinforcement observed for composite materials containing nanosized filler particles. It is well-known that the extremely high plateau modulus of such composite materials is due to a combination of different effects. These contributions can be partly quantified and separated based on the results of our study (Figure 11): (i)

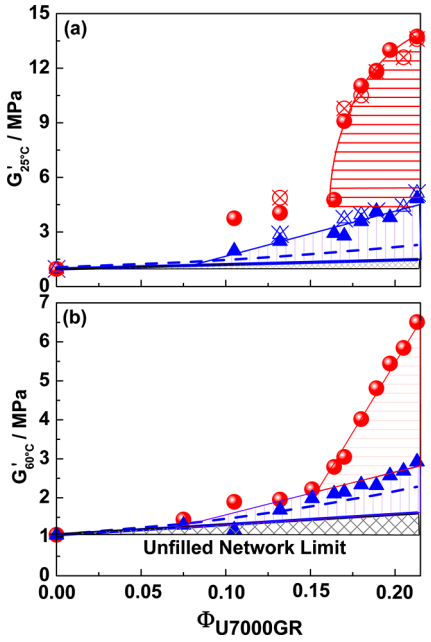

Figure 11. Comparison of extrapolated storage moduli at $\gamma \rightarrow 0$ (circles) and $\gamma \rightarrow \infty$ (triangles) for composites with different silica U7000GR content measured at (a) 25 °C and (b) 60 °C. Contributions of "filler network" (horizontal hatch), due to "glassy layer" and "occluded rubber" (vertical hatch) and hydrodynamic effects of the pure filler particles (cross hatch) are indicated. The thin solid line (unfilled network limit) is the plateau modulus of the unfilled rubbers $G_N^0(\phi = 0)$, and the thick solid line corresponds the prediction of the Einstein−Smallwood model $G'_{ES} = (1 + 2.5\phi)G_N^0(\phi = 0)$,[44,45] while the thick dashed line includes the $14.1\phi^2$ term derived by Guth and Gold.[46] Data for the composites containing U7000GR/BK3 mixtures (symbols with cross at center) are shown for comparison in (a).

Classical reinforcement contributions by solid particles with a volume fraction ϕ described by hydrodynamic models like those proposed by Einstein,[44] Smallwood,[45] and Guth−Gold[46] as well as more recently proposed modifications of these models.[9,47] (ii) Strong contributions of a so-called "filler network", i.e., a percolating solid phase incorporating the filler particles.[38,48,49] (iii) Potential contributions of an immobilized glassy fraction of the polymer matrix at the interface of the filler particles increasing the fraction of solid material and being important for the percolation of the "filler network".[9,50] (iv) Further contributions due to "occluded rubber" located within filler aggregates shielded from the shear field leading to hydrodynamic effects causing larger reinforcement.[40,51] Details depend on many factors in particular filler particle size, filler content, filler dispersion, aggregation behavior, and filler−matrix interaction.

Comparing values for the storage modulus G' from linear response measurements (γ = 0.2%) in the plateau range, theoretical predictions of the Einstein−Smallwood (ES) equation G'_{ES}, and G'_∞ and G'_0 values from strain sweeps in the range $0.001\% \leq \gamma \leq 20\%$, one can conclude that hydrodynamic contributions of the nanosized silica particles (i) alone are relatively small at 80 °C. This is not only true considering the minimum predicition of the hydrodynamic effect from ES (thick solid lines in Figure 11) but still valid for the "worst-case" estimate based on the equation by Guth and Gold[46] that includes an additional quadratic term $14.1\phi^2$ (thick dashed lines in Figure 11). All newer treatments to describe hydrodynamic effects concluded on a smaller prefactor.[9,47]

Contributions of the so-called "filler network" (ii) to the overall reinforcement can be quantified based on strain sweeps since the percolating solid phase can be destroyed by large-amplitude deformations γ>1% (cf. sketches shown as insets in Figure 8). This phenomenon is called Payne effect and can be nicely parametrized using the Kraus equation. The results for composites filled with U7000GR show a percolation threshold at a filler fraction of $\phi \approx 0.15$, i.e., a filler content of ≈55 phr (Figure 11). The threshold in SBR samples containing a mixture of nanosized silica and micrometer-sized BK3 particles seems to appear at similar silica U7000GR contents independent of the additional BK3 content. This indicates that the aggregation of the silica particles is not seriously affected by the existence of much larger filler particles.

An evaluation of the large-deformation limit of the strain sweeps G'_∞ measured at 25 °C shows that the G'_{ES} values predicted by the Einstein−Smallwood equation are not reached even if the filler network is practically destroyed (Figure 11). This indicates that there are additional contributions to reinforcement which should be due to an immobilized polymer fraction localized at surfaces of the filler particles (iii) and "occluded rubber" located within filler aggregates (iv). This extra reinforcement ($G'_\infty - G'_{ES}$) is obviously not depending on the total filler content ϕ. It depends basically on the U7000GR content and is not significantly changing if BK3 is added (Figure 11). The systematic increase of G'_∞ with U7000GR content in both investigated series I and II clearly indicates that the total surface area per unit composite is probably the most relevant parameter for extra reinforcement ($G'_\infty - G'_{ES}$). To a certain extent this effect might be due to a glassy polymer layer with a thickness of 1−2 nm located at the surface of the filler particles like observed for other systems based on calorimetric measurements,[52,53] an evaluation of shear,[49] and dielectric data[54] as well as solid-state NMR methods.[29,55] In the case of nanosized filler particles this thin glassy layer can increase the fraction of solid-like material $\phi_{solid} = \phi + \phi_{glassy\ layer}$ in the composites significantly (up to a few 10% for primary particle diameters of about 10−20 nm). Recent low-field NMR experiments support the existence of a glassy polymer layer in our samples, details of which will be the subject of a separate publication. As a main result, we find that the glassy fraction is only on the order of few percent of the polymer fraction at 25 °C, corresponding to an increase of the effective filler fraction by ∼10% for the composites investigated here. Considering the original Einstein−Smallwood approach as correct, the volume fraction of the solid material ϕ_{solid} should be 200% of the original filler content ϕ in order to explain the obtained G'_∞ values. It seems to be unrealistic from our current point of view to assume that the observed G'_∞ values can be explained by hydrodynamic effects of the filler particles or filler particles plus glassy layer alone, although more detailed hydrodynamic models[9,46,47] exist which predict higher reinforcement compared to the Einstein−Smallwood equation and precise estimates based on such models are impossible since certain assumptions are violated. Additional hydrodynamic effects (iv), which are related to the presence of larger filler aggregates existing also for large strains ($\gamma \gg \gamma_c$) where the filler network is destroyed, are obviously important. From a hydrodynamic point of view these aggregates may act like bigger objects containing "occluded" rubber shielded from

dx.doi.org/10.1021/ma300925p | Macromolecules 2012, 45, 6504−6515

the shear flow what leads finally to an effectively larger filler fraction and stronger reinforcement.[40,51]

An interesting aspect of our study is that the contributions of the "filler network" quantified by the step height in the storage modulus in strain sweeps $\Delta G'$ is more pronounced at 25 °C slightly above the glass transition of the rubber matrix but 50% reduced at high temperatures of 60 °C (Figure 11). This might be explained by a softening of a large fraction of the glassy layer at temperatures several 10 K above the glass temperature of bulk rubber. Although the glassy layer is only a small fraction of the entire polymer matrix, its influence on reinforcement can be tremendous since the glassy layer is possibly important for the percolation and the morphology of the solid phase.[56] Glassy layers have been also reported for polymer immobilized at the interface of nanosized silica particles and nanoporous silica materials where a second glass transition is seen in DSC scans or relaxation data.[53,57−59] A glassy polymer layer softening above T_g of the bulk rubber could consitently explain (i) temperature-dependent changes of $\Delta G'(\gamma)$ in strain sweeps and (ii) the systematic reduction of $G'(T)$ in the plateau range in linear response measurements for large filler contents (Figure 3). Note that strong changes in the percolation threshold are not observed although the load-carrying capacity of the solid cluster seems to be reduced at high temperature; i.e., the percolation thresholds at 25 and 60 °C are comparable (Figure 11). Significant changes due to an additional fraction of large BK3 particles are not observed. The behavior is obviously dominated by nanosized U7000GR silica particles. Simple models explaining reinforcement only based on hydrodynamic effects are proven wrong for the investigated model composites containing nanosized as well as micrometer-sized filler particles. Further studies by low-field NMR experiments to quantify the glassy layer content and systematic shear experiments focused on the influence of nonlinear deformations on the shear modulus in linear response experiments are required to come to a qualified understanding of the reinforcement effects and quantitative predictions.

Parameters Influencing the Energy Dissipation of Filled Elastomers. Another important issue is the dissipation of composite materials in different frequency−temperature ranges. This is an important parameter for the performance of tire treads made from nanoparticle elastomer composites. The results of our study can be used in particular to check which effects are important for the rolling resistance, which is in technical contexts often quantified by the loss tangent at 60 °C and 10 Hz although the physical dissipation measure is the value of the shear loss modulus G'' according to linear response theory. Figure 12 shows the values of G'' for composites with different filler fractions measured at 60 °C. The shear data for samples filled with different amounts of silica U7000GR as well as U7000GR/BK3 mixtures show consistently that the dissipation in the high temperature range increases strongly with increasing surface area of the filler system used. There might be two possible interpretations of this finding. (1) Following the interpretation discussed above, one would assume that the sequential softening of the glassy polymer layer in the temperature interval a few 10 K above the T_g of the bulk rubber (α' range) result not only in a decrease of G' with increasing temperature but also in an amplified dissipation G'' in the same range according to the Kramers−Kronig relations. In the framework of this picture an increasing surface area of the filler system leads to a systematic increase of the dissipation G'' as observed. (2) An alternative approach to explain this

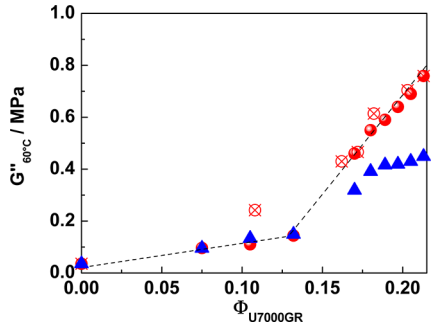

Figure 12. Loss modulus G'' at 60 °C for composites containing different amounts of silica U7000GR measured with small ($\gamma \approx 0.2\%$, circles) and large ($\gamma \approx 18\%$, triangles) strain amplitudes. Data from measurements on composites containing different U7000GR/BK3 mixtures are shown for comparison (symbols with cross at center).

trend is to assume that there is a dissipative mechanism incorporating filler particles or solidlike aggregates containing filler particles and glassy layer. Also in this case, an increasing surface area of the filler system would lead to an increasing dissipation. Both mechanisms may contribute to the high dissipation of filled elastomers containing nanosized particles. A recent simulation study indeed suggested that the dissipation is restricted to a very small, even subpercent fraction of the polymer material residing in "glassy" bridges.[56] Note that there are indications for the coexistence of two different dissipations mechanisms in the rubber plateau range. There is a change in the slope of log G'' (log ω) from power law behavior in the α' range to nearly constant low-frequency dissipation (Figures 4 and 6). Possibly softening processes in the polymer matrix dominate in the α' range while dissipative mechanisms incorporating filler aggregates are most important at low frequencies and high temperatures.

A comparison of the data in Figure 12 with Figure 11b shows that the dissipation G'' depends in a similar way on the filler fraction as the corresponding storage modulus G'. Again, the addition of BK3 particles has no large effect. For both quantities, G' and G'', filler effects are stronger above the percolation threshold at a silica U7000GR fraction of $\phi_{U7000GR} \approx 0.15$, indicating that reinforcement and increased dissipation are coupled. The exact relation between structure of the filler system and modulus, though, should be different for the storage and the loss modulus as indicated by the measurements presented in Figure 9 showing that a nonlinear deformation with a strain amplitude of $\gamma = 9\%$ leads to a strong reduction of G' while G'' is only weakly affected. This is also highlighted by the corresponding large-strain data shown in Figure 12.

In general, the results for composites containing variable amounts of fillers with different particle sizes may help to understand the molecular mechanisms contributing to dissipation in filled elastomers. A final understanding of such effects would be important for an efficient optimization of nanocomposites for many applications where dissipation is a main optimization criterion.

■ CONCLUSIONS

Systematic studies on solution styrene−butadiene rubber samples (Sprintan SLR-4602 - Schkopau) containing different amounts of silica as well as mixtures of nanoscopic U7000GR silica and microscopic BK3 filler particles show that the total surface area of the filler system per unit composite is of major

importance for the mechanical properties of such materials. Reinforcement and storage modulus in the rubber plateau region G_0^N as well as dissipation G'' in the plateau range depend basically on the U7000GR content and do not change significantly if additional BK3 particles are added. A combination of DQ NMR measurements on these composites with shear data for unfilled rubbers allows—for the first time—to estimate the cross-link density of the rubber matrix in composites in absolute units. The results show clearly that the cross-link density decreases systematically with increasing U7000GR filler content and total surface area of the filler system per unit composite. We interpret this as a consequence of a strong absorption of the cross-linking agent on the surface of filler particles. A detailed analysis of different effects contributing to reinforcement in composites indicates that the load-carrying capacity of the filler network decreases with increasing temperature. This can be concluded from strain sweeps performed at different temperatures as well as from temperature-dependent shear measurements in the plateau range. This is an interesting finding which may indicate that a glassy polymer fraction is incorporated in the solidlike "filler network" in case of silica particles. Since the glassy polymer should partly soften at higher temperature, a reduction of the reinforcement with temperature seems to be an expected finding. This can be explained by a reduced fraction of glassy polymer and a filler network at high temperatures which has a smaller load-carrying capacity. Additional contributions due to occluded rubber located in filler aggregates leading to extra hydrodynamic contributions to reinforcement due to an effectively higher solid content are indicated by a remaining difference between large-strain limit for the storage modulus from strain sweeps and predictions of the Einstein−Smallwood equations $G'_\infty - G'_{ES}$. Significant contributions of BK3 particles to reinforcement are not observed.

The dissipation in the plateau range, important for the rolling resistance of tires, is interestingly also dominated by the silica U7000GR content and the total surface area of the filler system per unit composite. There are indications that the high dissipation of composites in the plateau region has two different origins which both depend on the surface area of the filler system. Slightly above the conventional α process an additional α' process is observed which may reflect the softening process of a glassy polymer layer with nanoscopic dimensions located at the interfaces. The high, practically frequency-independent dissipation G'' at low frequencies and high temperatures >50 °C may reflect dissipative mechanisms incorporating solidlike aggregates contributing to the overall dissipation of the investigated composites. These observations for our model systems may help to understand different molecular and mesoscopic contributions to reinforcement and dissipation in filled elastomers which are of central importance in many fields of applications but in particular for the efficient optimization of tire treads being important for rolling resistance, fuel consumption, and CO_2 emission of cars.

APPENDIX. SHIFT FACTORS AND LOSS TANGENT CURVES

Master curves have been constructed for all investigated composites by horizontal shifting individual isotherms measured in the frequency range $0.1 \leq \omega \leq 100$ rad/s as discussed in the main text. Figure 13 shows the obtained shift factors a_T versus inverse temperature for two series of composites containing (a) different amounts of U7000GR as well as (b) mixtures of U7000GR and BK3 particles. Two different temperature regions are commonly observed for both series in these plots. In the α relaxation region ($T < 10$ °C) the shift factors of all samples are quite similar showing that the softening behavior of the major fraction of the polymer matrix is identical. In the rubber plateau region ($T > 10$ °C) the temperature dependence of the apparent shift factors a_T becomes stronger if the U7000GR content is increased. This trend and differences in the behavior compared to that in the α range might be interpreted as first indications for the existence of relaxation modes in the rubber plateau range (α', LFD) of

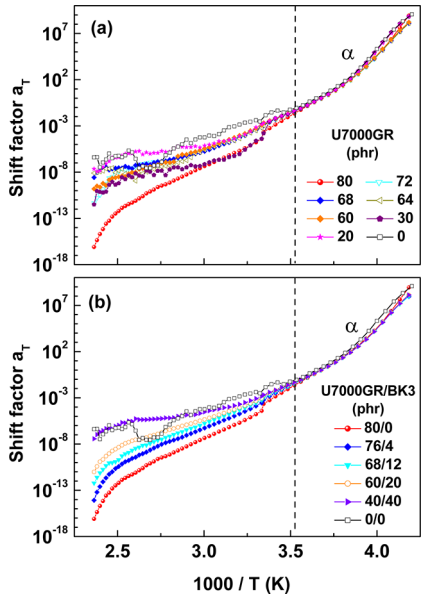

Figure 13. Horizontal shift factors a_T as a function of $1/T$ for composites containing (a) different amounts of silica U7000GR and (b) mixtures of silica and borosilicate particles. The reference temperature is 0 °C. The dashed lines indicate the lower limit of the α relaxation region at $T \approx 10$ °C.

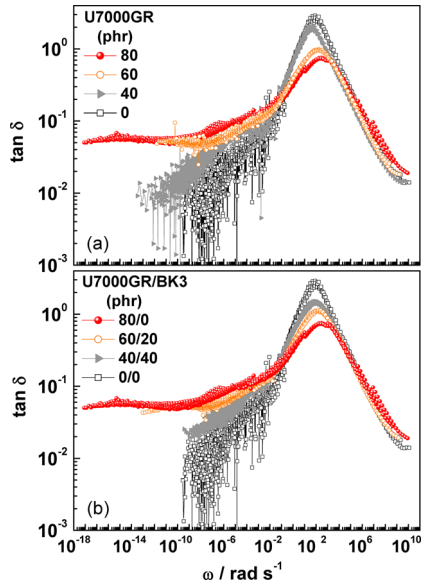

Figure 14. Master curves for the loss tangent tan δ as a function of log ω for composites containing (a) different amounts of silica U7000GR and (b) mixtures of silica and borosilicate particles. The reference temperature is 0 °C.

dx.doi.org/10.1021/ma300925p | Macromolecules 2012, 45, 6504−6515

composites with a significantly different temperature dependence. An additional fraction of BK3 particles does not change the trends significantly, showing a strong influence of the total surface area of the filler system per unit composite on the apparent shift factors a_T.

Loss tangent data from the master curve construction are presented in Figure 14. The maximum values tan δ_{max} in the α relaxation range depend significantly on the U7000GR content. The tan δ_{max} value decreases systematically with increasing U7000GR content while the frequency position of the tan δ peak maximum shifts to higher frequencies. The curves for larger silica contents also show that there are two regimes with different slope in the log tan δ vs log ω plots in the rubber plateau range. This confirms nicely the existence of different relaxation regimes (α', LFD) in the rubber plateau range as discussed in the main text.

AUTHOR INFORMATION

Corresponding Author

*E-mail: beiner@physik.uni-halle.de.

Notes

The authors declare no competing financial interest.

ACKNOWLEDGMENTS

The authors thank Dr. Uwe Ferner (TROVOTEC GmbH) and Dr. Sven Thiele (Styron Deutschland GmbH) for many fruitful discussions as well as for providing BK3 and Sprintan SLR-4602 - Schkopau, respectively, including detailed information about their properties. We acknowledge financial support of this work by the state Sachsen-Anhalt in the framework of the "Innovationscluster Polymertechnologie I" and funding by the Deutsche Forschungsgemeinschaft in the framework of research projects SA 982/6-1 (K.S.) and BE 2352/4-1 (M.B.).

REFERENCES

(1) Kraus, G. *Reinforcement of Elastomers*; Interscience Publishers: New York, 1965.
(2) *Science and Technology of Rubber*; Mark, J. E., Erman, B., Eirich, F. R., Eds.; Elsevier: Amsterdam, 2006.
(3) Medalia, A. I. Effects of Carbon Black on Abrasion and Treadwear. The Second international conference on carbon black, 1993; pp 295−304.
(4) Robertson, C.; Roland, C. *Rubber Chem. Technol.* **2008**, *81*, 506−522.
(5) Gerspacher, M.; O'Ferrell, C. P. *KGK* **2001**, *54*, 153−158.
(6) Schweitzer, C.; Frank, U. E.; Steiner, P. P.; Mruk, R.; Weiter, C. A. US 20110152434Al, 2011.
(7) Wang, M.-J. *KGK* **2007**, *60*, 438−443.
(8) Wang, M.-J. *KGK* **2008**, *61*, 33−42.
(9) Heinrich, G.; Klüppel, M.; Vilgis, T. A. *Curr. Opin. Solid State Mater. Sci.* **2002**, *6*, 195−203.
(10) Klüppel, M.; Heinrich, G. *Rubber Chem. Technol.* **2000**, *73*, 578−606.
(11) Persson, B. *J. Chem. Phys.* **2001**, *115*, 3840−3861.
(12) Persson, B. *Surf. Sci.* **1998**, *401*, 445−454.
(13) Angell, C. *Science* **1995**, *267*, 1924−1935.
(14) Böhmer, R.; Chamberlin, R.; Diezemann, G.; Geil, B.; Heuer, A.; Hinze, G.; Kuebler, S.; Richert, R.; Schiener, B.; Sillescu, H.; Spiess, H.; Tracht, U.; Wilhelm, M. *J. Non-Cryst. Solids* **1998**, *235−237*, 1−9.
(15) Donth, E. *The Glass Transition: Relaxation Dynamics in Liquids and Disordered Materials*; Springer: Heidelberg, 2001.
(16) Debenedetti, P. G.; Stillinger, F. H. *Nature* **2001**, *410*, 259−267.
(17) Berthier, L.; Biroli, G.; Bouchaud, J.; Cipelletti, L.; El Masri, D.; L'Hote, D.; Ladieu, F.; Pierno, M. *Science* **2005**, *310*, 1797−1800.
(18) McKenna, G. B. *Nat. Phys.* **2008**, *4*, 673−674.
(19) Dawson, K.; Kearns, K.; Yu, L.; Steffen, W.; Ediger, M. *Proc. Natl. Acad. Sci. U. S. A.* **2009**, *106*, 15165−15170.
(20) Ngai, K. *Relaxation and Diffusion in Complex Systems*; Springer: Heidelberg, 2011.
(21) Alcoutlabi, M.; McKenna, G. B. *J. Phys.: Condens. Matter* **2005**, *17*, R461−R524.
(22) Alba-Simionesco, C.; Coasne, B.; Dosseh, G.; Dudziak, G.; Gubbins, K.; Radhakrishnan, R.; Sliwinska-Bartkowiak, M. *J. Phys.: Condens. Matter* **2006**, *18*, R15−R68.
(23) Hempel, E.; Vieweg, S.; Huwe, A.; Otto, K.; Schick, C.; Donth, E. *J. Phys. IV* **2000**, *10*, 79−82.
(24) Beiner, M.; Huth, H. *Nat. Mater.* **2003**, *2*, 595−599.
(25) Ellison, C. J.; Torkelson, J. M. *Nat. Mater.* **2003**, *2*, 695−700.
(26) Dutcher, J.; Ediger, M. *Science* **2008**, *319*, 577−578.
(27) Serghei, A.; Tress, M.; Kremer, F. *J. Chem. Phys.* **2009**, *131*, 154904−+.
(28) Boucher, V.; Cangialosi, D.; Alegria, A.; Colmenero, J.; Gonzalez-Irun, J.; Liz-Marzan, L. *Soft Matter* **2010**, *6*, 3306−3317.
(29) Papon, A.; Saalwächter, K.; Schäler, K.; Guy, L.; Lequeux, F.; Montes, H. *Macromolecules* **2011**, *44*, 913−922.
(30) Saalwächter, K. *Prog. Nucl. Magn. Reson. Spectrosc.* **2007**, *51*, 1−35.
(31) Valentin, J.; Mora-Barrantes, I.; Carretero-Gonzalez, J.; Lopez-Manchado, M.; Sotta, P.; Long, D.; Saalwächter, K. *Macromolecules* **2010**, *43*, 334−346.
(32) Styron GmbH, SPRINTAN SLR 4602 - Schkopau, Technical information 2010, Form No. 850-00901.
(33) Evonik GmbH, Ultrasil U7000GR - Technical information.
(34) Ferner, U. *Datenblatt TROVOpowder BK3* **2010**.
(35) Keller, M.; Wutzler, A.; Mujtaba, A.; Le, H. H.; Ilisch, S.; Radusch, H.-J. Proceedings of Symposium "Polymer Blends and Nanocomposites with Biobased Components", 14−15 Sept 2011, Halle (Saale), ISBN 978-3-86829-391-3.
(36) Valentin, J.; Posadas, P.; Fernandez-Torres, A.; Malmierca, M.; Gonzalez, L.; Chasse, W.; Saalwächter, K. *Macromolecules* **2010**, *43*, 4210−4222.
(37) Rubinstein, M.; Colby, R. H. *Polymer Physics*; Oxford University Press: Oxford, 2003.
(38) Payne, A. R. *J. Appl. Polym. Sci.* **1962**, *6*, 57−63.
(39) Kraus, G. *J. Appl. Polym. Sci.: Appl. Polym. Symp.* **1984**, *39*, 75−92.
(40) Robertson, C. G.; Bogoslovov, R.; Roland, C. M. *Rubber Chem. Technol.* **2009**, *82*, 202−213.
(41) Jouault, N.; Vallat, P.; Dalmas, F.; Said, S.; Jestin, J.; Boue, F. *Macromolecules* **2009**, *42*, 2031−2040.
(42) Medalia, A. *Rubber Chem. Technol.* **1978**, *51*, 437−523.
(43) Wang, M. J. *Rubber Chem. Technol.* **1998**, *71*, 520−589.
(44) Einstein, A. *Ann. Phys.* **1906**, 289−306.
(45) Smallwood, H. M. *J. Appl. Phys.* **1944**, *15*, 758−766.
(46) Guth, E.; Gold, O. *Phys. Rev.* **1938**, *53*, 322.
(47) Vilgis, T. A.; Heinrich, G.; Klüppel, M. *Reinforcement of Polymer Nano-composites*; Cambridge University Press: New York, 2009.
(48) Klüppel, M.; Schuster, R. H.; Heinrich, G. *Rubber Chem. Technol.* **1997**, *70*, 243−255.
(49) Berriot, J.; Montes, H.; Lequeux, F.; Long, D.; Sotta, P. *Europhys. Lett.* **2003**, *64*, 50−56.
(50) Merabia, S.; Sotta, P.; Long, D. R. *Macromolecules* **2008**, *41*, 8252−8266.
(51) Medalia, A. I. *Rubber Chem. Technol.* **1972**, *45*, 1171−1194.
(52) Vieweg, S.; Unger, R.; Hempel, E.; Donth, E. *J. Non-Cryst. Solids* **1998**, *235−237*, 470−475.
(53) Sargsyan, A.; Tonoyan, A.; Davtyan, S.; Schick, C. *Eur. Polym. J.* **2007**, *43*, 3113−3127.
(54) Fragiadakis, D.; Pissis, P.; Bokobza, L. *J. Non-Cryst. Solids* **2006**, *352*, 4969−4972.
(55) Berriot, J.; Montes, H.; Lequeux, F.; Long, D.; Sotta, P. *Macromolecules* **2002**, *35*, 9756−9762.
(56) Gusev, A. A. *Macromolecules* **2006**, *39*, 5960−5962.

(57) Arndt, M.; Stannarius, R.; Groothues, H.; Hempel, E.; Kremer, F. *Phys. Rev. Lett.* **1997**, *79*, 2077−2080.
(58) Rengarajan, G. T.; Enke, D.; Steinhart, M.; Beiner, M. *J. Mater. Chem.* **2008**, *18*, 2537−2539.
(59) Papon, A.; Montes, H.; Hanafi, M.; Lequeux, F.; Guy, L.; Saalwächter, K. *Phys. Rev. Lett.* **2012**, *108*, 065702.